Sound absorption characteristics of a double-leaf structure with an MPP and a permeable membrane

Sakagami, Kimihiro
Fukutani, Yusaku
Yairi, Motoki
Morimoto, Masayuki

(Citation)
Applied Acoustics,76:28-34

(Issue Date)
2014-02

(Resource Type)
journal article

(Version)
Accepted Manuscript

(URL)
https://hdl.handle.net/20.500.14094/90001916

Sound absorption characteristics of a double-leaf structure with an MPP and a permeable membrane

Kimihiro Sakagami*, Yusaku Fukutani, Motoki Yairi**, Masayuki Morimoto

Environmental Acoustics Laboratory, Department of Architecture,
Graduate School of Engineering, Kobe University,
Rokko, Nada, Kobe, 657-8501 Japan

*Corresponding author: saka@kobe-u.ac.jp

** Kajima Technical Research Institute, Tobitakyu, Chofu, 182-0036 Tokyo, Japan

Keywords: Microperforated panel, permeable membrane, honeycomb, space absorber, sound absorption

ABSTRACT

As for the sound absorbing system using an MPP (microperforated panel), a double-leaf MPP sound absorber has been studied so far. However, this structure uses two MPPs, which are still expensive, and is disadvantageous when its cost is concerned. Therefore, it is considered that it can be advantageous if one of the leaves can be replaced with a less expensive material keeping high sound absorption performance. In this study, the possibility of producing a useful sound absorbing structure with an MPP and a permeable membrane as an alternative less expensive material is examined. The acoustic properties of this MPP and permeable membrane combination absorber are analysed theoretically with a Helmholtz integral formulation. The absorption performance and mechanism are discussed through the numerical examples. Also, the effect of a honeycomb in the air cavity, which is to be used for reinforcing the structure, is also discussed through a theoretical analysis.

1. INTRODUCTION

For sound absorption treatment in architectural and building acoustical purposes, porous and fibrous absorbents are most widely used. However, porous and fibrous absorbents have various shortcomings in the health problems, durability, and recyclability, etc.. As an alternative sound absorbing material, so-called next-generation sound absorbing materials have been studied so far. There have been proposed many types of next-generation sound absorbing materials including an MPP (microperforated panel) [1-4] and a permeable/impermeable membrane [5-10]. The MPP is one of the most promising alternatives among those next-generation sound absorbers. MPPs are usually used being placed with a rigid-back wall with an air-cavity in-between, and shows the Helmholtz-type resonance absorption with its perforations and the cavity. It is also known that a double-leaf MPP, using two leaves of MPP, with a back wall shows wider and more efficient sound absorption [1,2,11]. There are many studies on various applications of MPPs [11-15].

The sound absorbing structure using two MPP leaves is already employed in various practical situations, however, MPPs are still expensive and are therefore disadvantageous when the cost is concerned. Considering this problem, it can be useful and advantageous, if one of its two MPP leaves with another less expensive material, and if it can be possible to construct an efficient sound absorber with it.

So far the authors have studied a double-leaf panel-like space sound absorber with an MPP and a permeable membrane [16], and show that this structure offers somewhat better sound absorption performance than a double-leaf MPP space sound absorber (DLMPP) [17,18]. However, the same studies only consider the case of a space sound absorber, and it is not discussed in the case of an absorber with a rigid-back wall, which is more general usage.

In this study, a sound absorbing structure with an MPP and a permeable membrane with a rigid-back wall and air-cavities in between is theoretically analysed to derive its sound absorption characteristics and to discuss its sound absorption mechanism. Also, the effect of a honeycomb in its air-cavities is discussed with theoretical analysis: the honeycomb in the cavity is found to improve not only its structural strength but also its sound absorption performance [19, 20]. A discussion is made through the numerical examples.

2. THEORETICAL CONSIDERATIONS

2.1 Model for analyses

The model for analyses of a double-leaf sound absorbing structure with an MPP and a permeable membrane (PM) with a rigid-back wall and air cavities is shown in Figs. 1 and 2. Two alternative combinations are shown in these figures: In Fig. 1 the case with an MPP on the illuminated side (MPP-PM absorber) is shown and in Fig. 2 that with a PM on the illuminated side (PM-MPP structure) is shown. The rigid-back wall is in *x-y* plane, and both the MPP and PM, as well as the back wall are all of infinite extent. The incidence wave is a plane wave of unit pressure amplitude and impinges at the angle of incidence θ. The parameters of the MPP are: thickness t, hole diameter d, perforation ratio p. The flow resistance and the tension of the PM are R and T, respectively. The first leaf (either MPP or PM on the illuminated side, i.e., left hand side) is assumed to have the surface density, acoustic impedance and vibration displacement of M_1, Z_1, $w_1(x)$, respectively. For the second leaf (either MPP or PM in the middle, i.e., right hand side), they are assumed to be M_2, Z_2, $w_2(x)$, respectively. The

depths of the air cavities 1 and 2 are D_1 and D_2, respectively. The time factor $\exp(-i\omega t)$ is suppressed throughout. All impedances in the analyses are normalised to $\rho_0 c_0$: ρ_0 is air density (1.2[kg/m^3]) and c_0 is the sound speed in the air (340[m/s]).

According to Maa's theory [2], the acoustic impedance of the MPP, Z_{MPP}, is expressed with its acoustic resistance r and the acoustic reactance ωm, as follows:

$$Z_{MPP} = r - i\omega m \tag{1}$$

$$r = \frac{32\eta t}{p\rho_0 c_0 d^2}\left(\sqrt{\frac{K^2}{32}+1}+\frac{\sqrt{2}}{8}K\frac{d}{t}\right) \tag{2}$$

$$\omega m = \frac{\omega t}{pc}\left(1+\frac{1}{\sqrt{9+K^2/2}}+0.85\frac{d}{t}\right) \tag{3}$$

where, $$K = d\sqrt{\frac{\omega\rho_0}{4\eta}} \tag{4}$$

The acoustic impedance of the PM, Z_{PM}, is expressed by

$$Z_{PM} = \frac{R}{\rho_0 c_0} \tag{5}$$

where, ω is the angular frequency, η is the viscosity coefficient (1.789×10^{-5}[Pa s]). The acoustic impedance of the PM in the above is that in the case of immovable membrane, i.e., the sound induced vibration of the membrane is here not taken into account: the sound induced vibration is considered later by making the equation of sound field interacted with that for vibration.

2.2 Analysis based on Helmholtz-Kirchhoff integral

In this section the theoretical analysis in the case with an MPP on the illuminated side (MPP-PM structure: Fig. 1) is presented. The following formulation is easily applied to the case with a PM on the illuminated side (PM-MPP structure: Fig. 2).

The surface sound pressure on the illuminated side surface of the MPP is expressed by a Helmholtz-Kirchhoff integral as follows:

$$p_1(x,0) = 2p_i(x,0) + \frac{i}{2}\int_{-\infty}^{\infty}\frac{\partial p_1(r_0)}{\partial n}H_0^{(1)}(k_0|x-x_0|)dx_0 \tag{6}$$

where, p_i is the pressure of the incidence wave, n the outward normal, $H_0^{(1)}$ is the first-kind Hankel function of zero order. The boundary condition on this surface is:

$$\frac{\partial p_1(r_0)}{\partial n} = \rho_0\omega^2 w_1(x_0) + iA_{m1}k_0\Delta P_1(x_0) \tag{7}$$

Here, $A_{m1}=\rho_0 c_0/Z_1$, k_0 is the wavenumber, ΔP_1 is the difference of the pressure of the both sides of the

MPP. From these equations, the sound pressure on the illuminated side surface of the MPP is expressed as follows:

$$p_1(x,0) = 2p_i(x,0) + \frac{i}{2}\int_{-\infty}^{\infty}[\rho_0\omega^2 w_1(x_0) + iA_{m1}k_0 p_1(x_0,0)]H_0^{(1)}(k_0|x-x_0|)dx_0 \tag{8}$$

The sound pressure and the particle velocity in the regions [II] and [III] are expressed as follows, according to the general form for the solution of a plane wave:

$$p_{2,3}(x,z) = (X_{2,3}e^{ik_0 z\cos\theta} + Y_{2,3}e^{-ik_0 z\cos\theta})e^{ik_0 x\sin\theta} \tag{9}$$

$$v_{2,3}(x,z) = \frac{\cos\theta}{\rho_0 c_0}(X_{2,3}e^{ik_0 z\cos\theta} - Y_{2,3}e^{-ik_0 z\cos\theta})e^{ik_0 x\sin\theta} \tag{10}$$

where $X_{2,3}$ and $Y_{2,3}$ are the pressure amplitude of the propagating wave going to +z and –z directions, respectively. Here, when a honeycomb is inserted in the cavities, the sound waves in the cavities propagates only into +/- z directions (θ=0) only, and θ=0 should be substituted in the terms in ( ) of eqns. (9) and (10).

The boundary conditions are as follows:

$$v_2(x,0) = -i\omega w_1(x) + \frac{\Delta P_1(x)}{Z_1} \tag{11}$$

$$v_2(x,D_1) = -i\omega w_2(x) + \frac{\Delta P_2(x)}{Z_2} \tag{12}$$

$$v_3(x,D_1) = -i\omega w_2(x) + \frac{\Delta P_2(x)}{Z_2} \tag{13}$$

$$v_3(x,D_1+D_2) = 0 \tag{14}$$

where ΔP_2 is the difference of the sound pressure of the both sides surfaces of the PM.

From eqns. (11)…(14), $X_{2,3}$ and $Y_{2,3}$ are obtained. The sound pressure on the transmitted (back) side surface of the MPP is obtained from X_2 and Y_2. The sound pressure on the illuminated (left) side surface of the PM is obtained from X_3 and Y_3.

The vibration displacements of the MPP and PM $w_{1,2}(x)$ are obtained by using the unit response of the leaves $u_{1,2}(x)$ as follows:

$$w_1(x) = \int_{-\infty}^{\infty}[p_1(\xi,0) - p_2(\xi,0)]u_1(x-\xi)d\xi \tag{15}$$

$$w_2(x) = \int_{-\infty}^{\infty}[p_2(\xi,D_1) - p_3(\xi,D_1)]u_2(x-\xi)d\xi \tag{16}$$

Using Fourier transform technique, the above equations can be solved in the wavenumber space. Here, Fourier transform and inverse transform are defined as follows:

$$F(k)=\frac{1}{2\pi}\int_{-\infty}^{\infty} f(x)e^{-ikx}dx \tag{17}$$

$$f(x)=\int_{-\infty}^{\infty} F(k)e^{ikx}dk \tag{18}$$

The solution obtained by solving the above equations using Fourier transform technique, the final form of the reflected pressure is obtained as follows:

$$p_r(x,z)=\left[1+\frac{i\rho_0\omega^2\Gamma_1(k_0\sin\theta)-k_0A_{m1}\Theta_1\{A_1\Gamma_1(k_0\sin\theta)+A_2\Gamma_2(k_0\sin\theta)+A_3\}}{k_0\cos\theta}\right]\ e^{i[k_0x\sin\theta-k_0z\cos\theta]} \tag{19}$$

where $\Gamma_{1,2}$, $\Theta_{1,2}$ and $A_{1,2,3}$ are the functions including the acoustic impedances of the MPP and PM and cavity depths, which are expressed as follows:

$$\Gamma_1(k)=\frac{-\Phi_1A_3+\Phi_1\Phi_2A_3B_2-\Phi_1\Phi_2A_2B_3}{-1+\Phi_1A_1+\Phi_1\Phi_2A_2B_1+\Phi_2B_2-\Phi_1\Phi_2A_1B_2}$$

$$\Gamma_2(k)=\frac{-\Phi_1\Phi_2A_3B_1-\Phi_2B_3+\Phi_1\Phi_2A_1B_3}{-1+\Phi_1A_1+\Phi_1\Phi_2A_2B_1+\Phi_2B_2-\Phi_1\Phi_2A_1B_2}$$

$\Phi_1=2\pi U_1(k)\Theta_1,\quad \Phi_2=2\pi U_2(k)\Theta_2$

$\Theta_1=\frac{1}{2EK},\quad \Theta_2=\frac{1}{-K}$

$A_1=2(I_2-L)EJ_2+I_1J_1J_2+I_1K$

$A_2=-(I_2-I_3)(K+J_1J_2)-2EI_1J_2$

$A_3=-4EJ_2$

$B_1=2E(I_2-L)+I_1J_1$

$B_2=-2EI_1-(I_2-I_3)J_1$

$B_3=-4E$

$C_1=(e^{i\varphi}-e^{-i\varphi})\cos\theta,\quad C_2=(e^{2i\varphi}-e^{2i(\varphi+\sigma)})\cos\theta$

$E=\frac{\rho_0c_0}{C_1Z_1},\quad F_1=\frac{\rho_0c_0}{C_1Z_2},\quad F_2=\frac{\rho_0c_0}{C_2Z_2}$

$G=i\rho_0c_0\omega$

$H_1=e^{i\varphi}+e^{-i\varphi},\quad H_2=e^{2i\varphi}+e^{2i(\varphi+\sigma)}$

$I_1=\frac{2G}{C_1},\quad I_2=\frac{H_1G}{C_1},\quad I_3=\frac{H_2G}{C_2}$

$J_1=1-EH_1+M,\quad J_2=1-F_1H_1+F_2H_2$

$K=4EF_1-J_1J_2$

$L=\frac{i\rho_0\omega^2}{\sqrt{k_0^2-k^2}},\qquad M=\frac{k_0A_{m1}}{\sqrt{k_0^2-k^2}}$

$\varphi=k_0D_1\cos\theta,\qquad \sigma=k_0D_2\cos\theta$

where $U_{1,2}(k)$ are the Fourier transforms of $u_{1,2}(x)$ and expressed as follows. In this case, $U_1(k)$ is the transformed unit response of the MPP, and $U_2(k)$ is that of the PM.

$$U_1(k)=\frac{1}{2\pi(Dk^4-\rho t\omega^2)};\quad D=\frac{Et^3(1-i\eta_P)}{12(1-\nu^2)} \tag{20}$$

$$U_2(k)=\frac{1}{2\pi(Tk^2-M_2\omega^2)} \tag{21}$$

where ρ, E, η_P, ν, and D are the density, Young's modulus, loss factor, Poisson's ratio and bending stiffness of the MPP, respectively.

As for the MPP (in this case it is assumed to be an elastic plate), the effect of the bending vibration, such as coincidence effect, is known to be negligible in the sound absorption [16, 18], it is neglected hereafter and approximated by the following equation:

$$U_1(k)=\frac{1}{2\pi(-M_1\omega^2)} \tag{22}$$

Regarding the PM, the effect of the tension T is known to be negligible in the case of infinite extent [5], the tension is neglected, i.e., T=0 is applied hereafter.

The absorption coefficient is obtained from the reflected pressure as follows:

$$\alpha_\theta=1-\left|p_r\right|^2 \tag{23}$$

The field-incidence-averaged sound absorption coefficient α is obtained by taking the average of α_θ from 0 to 78 degrees of the incidence angle.

$$\alpha=\frac{\int_{0°}^{78°}\alpha_\theta\sin\theta\cos\theta d\theta}{\int_{0°}^{78°}\sin\theta\cos\theta d\theta} \tag{24}$$

If the absorbing surface is rather small and used as a space absorber, it can be more reasonable to average from 0 to 90 degrees. However, in the preliminary studies, no significant difference was found between 78 and 90 degrees, therefore, in this paper averaging to 78 degrees (field-incidence-averaged value) is consistently used unless otherwise noted.

3. SOUND ABSORPTION CHARACTERISTICS IN THE CASE WITH AN MPP ON THE ILLUMINATED SIDE (MPP-PM STRUCTURE)

3.1 General discussion

The main features of the sound absorption characteristics of the MPP-PM structure (Fig. 1) are summarised in this section. In order to detailed discussion the characteristics are compared with those of the sound absorbing structures shown in Fig. 3.

An example of the calculated result is shown in Fig. 4. The parameters of the MPP and PM are both typical values: the thickness (t), hole diameter (d), perforation ratio (p) and surface density (M_{MPP}) of the MPP are 0.3 [mm], 0.3 [mm], 1.0 [%] and 1.0 [kg/m^2], respectively. The flow resistance (R) and surface density (M_{PM}) of the PM are 816 [Pa s/m] and 1.0 [kg/m^2], respectively. The depths of the air cavities between the MPP and PM (D_1) and between PM and the rigid-back wall (D_2) are both 50 [mm].

In Fig. 4, the MPP-PM structure shows the characteristics of a resonance type absorber, which is very similar to the single-leaf wall-backed MPP absorber. At low frequencies, 31.5 … 125 Hz, the absorption coefficient is low, and at middle frequencies, 125 … 1 kHz, the coefficient drastically increases reaching a significant peak of 0.8…0.9 at around 1 kHz. Above the peak frequency the coefficient steeply decreases. A couple of peaks appear at around 4 and 8 kHz, but these are rather small: these are considered to be caused by the higher order resonance of the system. As they are very sharp and dependent on the angle of incidence, in the case of field-incidence-averaged value, they become very low as is averaged. Therefore, in practice these peaks are not significant in sound absorption performance.

Comparing this example with a common double-leaf (wall-backed) MPP absorber, the width of the absorption frequency range is almost the same. Regarding the peak value, the proposed structure with a PM shows higher value than a common double-leaf MPP. When it is compared with a common single-leaf (wall-backed) MPP absorber, it can be stated that the characteristics are much improved, both in the absorption frequency range and the peak value, by using a PM.

3.2 Sound absorption mechanism

Here the sound absorption mechanism of the MPP-PM structure is discussed in comparison with the characteristics of a common single-leaf (wall-backed) absorber. To make the discussion clear and simple, the discussion is limited to the normal incidence case. All the parameters are the same as those in Fig. 4. For the reference, the sound absorbing structures compared for the discussion are shown in Fig. 5.

The calculated result is shown in Fig. 6. From this example, the increase at low to mid frequencies (lower than 500 Hz) shows similar value to that in the case of the single-leaf with an air cavity of 100 [mm] deep (Fig. 5(b)). The peak frequency is also similar to the same case. At high frequencies (above 1 kHz) the peaks of higher order resonances are similar to the case of the single-leaf with an air cavity of 50 [mm] deep (Fig. 5 (c)). On the other hand, the value of the absorption coefficient of the MPP-PM structure is higher than the other structures.

From the above discussion, the MPP-PM structure shows the following features: The absorption caused between the MPP and the back wall with 100 [mm] deep cavity contributes to mainly the low frequency characteristics of the present structure. On the other hand, that caused between the MPP and PM with 50 [mm] deep cavity contributes to mainly the mid to high frequency characteristics of the present structure. As the values around the peak are higher than a common single-leaf structure used to comparison here, the PM contributes to make the peak higher and efficient absorption.

4. SOUND ABSORPTION CHARACTERISTICS IN THE CASE WITH AN PM ON THE ILLUMINATED SIDE (PM-MPP STRUCTURE)

4.1 General discussion

The main features of the sound absorption characteristics of the PM-MPP structure (Fig. 2) are summarised in this section. In order to detailed discussion the characteristics are compared with those of the sound absorbing structures shown in Fig. 7.

An example of the calculated result is shown in Fig. 8. The parameters of the MPP and PM are the same as those in Fig. 4. From Fig. 8, it is observed that the PM-MPP structure shows porous-like

absorption characteristics in which a typical feature of a PM clearly appears: At low frequencies the absorption coefficient is low. At middle frequencies (125…1kHz) the value drastically increases, and in this example, a peak of around 0.85 appears at around 750…1kHz. The value decreases to about 0.7 above the peak frequency, and fluctuates between 0.6 and 0.75 up to 4 kHz. Thus, the sound absorption performance of this system is improved than a common double-leaf MPP absorber (with a back-wall), especially the difference is significant at high frequencies. On the other hand, when this absorber is compared with a single-leaf PM absorbing structure, there is little difference in their sound absorption performance, which means that the contribution of the MPP is very little. In other words, single PM sound absorbing structure is of somewhat good sound absorbing performance, and in such a case with a PM on the illuminated side the use of MPP can be said to be almost useless.

4.2 Sound absorption mechanism

Here the sound absorption mechanism of the PM-MPP structure is discussed in comparison with the characteristics of a common single-leaf (wall-backed) PM absorber. To make the discussion clear and simple, the discussion is again limited to the normal incidence case. All the parameters are the same as those in Fig. 4. For the reference, the sound absorbing structures compared for the discussion are shown in Fig. 9.

An example of the calculated result is presented in Fig. 10. From this example, the increase from low to mid frequencies (below 500 Hz) is almost completely in agreement with that in the case of the air cavity depth 100 [mm] (Fig. 9(b)). At high frequencies (above 2 kHz) it is not only very similar to that in the case of air cavity depth 50 [mm] (Fig. 9(c)), but also almost agrees quantitatively. On the other hand, in any case, the characteristics differ at middle frequencies.

From the discussion above, the absorption mechanism of the PM-MPP structure is interpreted as follows: At low frequencies the characteristics are close to those of air cavity depth 100 [mm], which means that the absorption taking place between the PM and rigid-back wall is dominant. At high frequencies the characteristics are close to those of air cavity depth 50 [mm], which means that the absorption taking place between the PM and MPP is dominant. In that, the contribution of the PM is large and that of the MPP is small.

5. EFFECT OF THE HONEYCOMB IN THE CAVITY

In the previous studies [19, 20] it is shown that the honeycomb in the air cavity of an MPP sound absorbers has an effect to increase the peak absorption and to broaden the absorption frequency range. Here, expecting the mechanical reinforcement of the present proposed sound absorption structures and the improvement of the sound absorption performance, the sound absorption characteristics of the honeycomb inserted cases are discussed. In this section all the results are calculated under field-incidence-averaged condition.

5.1 The case with an MPP on the illuminated side (MPP-PM structure)

The effect of a honeycomb in the air cavity is discussed in the case of the sound absorbing structure with an MPP on the illuminated side (MPP-PM structure: Fig. 1). For reference the comparison is made with the characteristics of the sound absorbing structures in Fig. 11.

Calculated results are shown in Fig. 12. Comparing the case with a honeycomb in the air

cavity D_1 (Fig. 11(b)) and that without a honeycomb (Fig. 11(a)), it is observed that the peak shifts to lower frequencies and becomes lower. In the previous studies [19, 20], it is not observed the peak to decrease by the effect of a honeycomb. Therefore, this decrease of the peak is a feature particular to the sound absorber of this type. This is inferred that the resonance peak becomes lower due to the PM which damps the standing wave in the air cavity. This problem needs further study and will be a subject of the sequels. Sound absorbing frequency range also does not show significant difference: it is not much different from that of the case without a honeycomb (Fig. 11(a)).

On the other hand, in the case of inserting a honeycomb in the air cavity D_2 (Fig. 11(c)), the result is different from that presented above: Comparing it with the result without a honeycomb (Fig. 11(a)), the peak shifts to lower frequencies and increases as reported in the previous studies [19, 20]. The absorption frequency range also changes and becomes wider.

In the case inserting honeycombs in the both air cavities, D_1 and D_2 (Fig. 11(d)), the peak shifts to lower frequencies and becomes higher, as well as, the absorption frequency range becomes wider than the case without a honeycomb (Fig. 11 (a)). However, the change is smaller than that in the case of a honeycomb in the air cavity D_2 only (Fig. 11(c)). This is because, as mentioned above, the effect of the honeycomb in the air cavity D_1 which deteriorates the peak absorption, and this cancels out the effect of the honeycomb in the air cavity D_2.

5.2 The case with a PM on the illuminated side

The effect of a honeycomb in the air cavity is discussed in the case of the sound absorbing structure with a PM on the illuminated side (Fig. 2). For reference the comparison is made with the characteristics of the sound absorbing structures in Fig. 13.

Calculated example is presented in Fig. 14. In the case with a honeycomb in the air cavity D_1 (Fig. 13(f)) the absorption coefficient increases and the frequency range becomes wider than that without a honeycomb (Fig. 13(e)). In the case with a honeycomb in the air cavity D_2 (Fig. 13(g)) the absorption frequency range broadens to lower frequencies and the absorptivity increases, though the difference is small at higher frequencies.

In the case with honeycombs inserted in the both air cavities D_1 and D_2 (Fig. 13(h)), the absorption frequency range becomes wider and the absorptivity becomes higher than that without a honeycomb, which is similar to the case with a honeycomb in the air cavity D_1 (Fig. 13(f)). Particularly, regarding the absorption frequency range, in this case the honeycombs show the most significant effect.

6. CONCLUDING REMARKS

In this study, the sound absorption characteristics of a double-leaf structure composed of an MPP and a permeable membrane (PM) with a rigid-back wall are theoretically studied, and discussed through the numerical examples.

In the case with an MPP on the illuminated side, the characteristics become quite similar to those of a common single-leaf MPP absorber with a back wall, showing the typical feature of resonance type absorption at middle frequencies. Regarding the absorption mechanism of this type, it is considered that the low frequency absorption is mainly caused between the MPP and back wall, and that the mid to high frequency absorption is mainly caused between the MPP and PM. The chief effect of the PM in this case greatly appears as the increase of the peak absorption and the broadening of the absorption frequency range.

In the case with a PM on the illuminated side, the characteristics are dominated by those of the PM, which results in the absorption characteristics similar to a porous absorbent which produces high absorptivity at mid to high frequencies. At low to mid frequencies, the characteristics are mainly dominated by the absorption caused between the PM and back wall, whilst the absorption caused between the PM and MPP is dominant at mid to high frequencies. The contribution of the MPP to the total absorption is very small: it only appears at mid to high frequencies.

From the above, although the absorption structure with a double-leaf of an MPP and PM with rigid back wall can be efficient when the PM is on the illuminated side, in this case the MPP does not contribute to the total absorption and is almost useless. On the other hand, when the MPP is on the illuminated side, the absorption performance of the MPP is greatly improved by the PM, which is considered to be efficient.

Regarding the use of the honeycomb in the air cavities of the absorption structure of these types, in both cases, i.e., the cases with an MPP on the illuminated side and with a PM on the illuminated side, the improvement of the absorption performance is observed as reported in the previous works. However, in the case with the MPP on the illuminated side, when a honeycomb is inserted in the air cavity of just behind the MPP, the absorptivity deteriorates by the effect of the honeycomb, which is a very particular result to this type of the absorption structure.

Acknowledgements

This work was in part supported by the Grant-in-Aid in Scientific Research (C, 20560550) from JSPS, Japan.

References

[1] Maa D-Y. Theory and design of microperforated panel sound-absorbing construction. Scientia Sinica 1975; 18: 55-71.
[2] Maa D-Y. Microperforated-panel wideband absorber. Noise Control Eng. J. 1987; 29:77-84.
[3] Maa D-Y. Potential of microperforated panel absorber. J. Acoust. Soc. Am. 1998; 104: 2861-2866.
[4] Maa D-Y. Practical single MPP absorber. International Journal of Acoust. and Vibration 2007; 12: 3-6.
[5] Sakagami K, Morimoto M, Takahashi D. A note on the acoustic reflection of an infinite membrane. Acustica 1994; 80: 569-572.
[6] Takahashi D, Sakagami K, Morimoto M. Acoustic properties of permeable membranes. J. Acoust. Soc. Am. 1996; 99: 3003-3009.
[7] Sakagami K, Kiyama M, Morimoto M, Takahashi D. Detailed analysis of acoustic properties of a permeable membrane. Applied Acoustics 1998; 54: 93-111.
[8] Kiyama M, Sakagami K, Tanigawa M, Morimoto M. A basic study on acoustic properties of double-leaf membranes. Applied Acoustics 1998; 54: 239-254.
[9] Sakagami K, Kiyama M, Morimoto M. Acoustic properties of double-leaf membranes with a permeable leaf on sound incidence side. Applied Acoustics 2002; 63: 911-922.
[10] Sakagami K, Uyama T, Morimoto M, Kiyama M. Prediction of the reverberation absorption coefficient of finite-size membrane absorbers. Applied Acoustics 2005; 66: 653-668.
[11] Asdrubali F, Pispola G. Properties of transparent sound-absorbing panels for use in noise barriers. J. Acoust. Soc. Am. 2007; 121: 214-221.
[12] Fuchs HV, Zha X. Acrylic-glass sound absorbers in the plenum of the Deutscher Bundestag.

Applied Acoustics 1997; 51: 211-217.
[13] Dupont T, Pavic G, Laulagnet B. Acoustic properties of lightweight micro-perforated plate systems. Acustica /Acta Acustica 2003; 89: 201-212.
[14] Kang J, Brocklesby MW. Feasibility of applying micro-perforated absorbers in acoustic window systems. Applied Acoustics 2005; 66: 669-689.
[15] Wu MQ. Micro-perforated panels for duct silencing. Noise Control Eng. J. 1997; 45: 69-77.
[16] Sakagami K, Nakamori T, Morimoto M, Yairi M. Absorption characteristics of a space absorber using a microperforated panel and a permeable membrane. Acoust. Sci. & Tech. 2011; 32: 47-49.
[17] Sakagami K, Morimoto M, Koike W. A numerical study of double-leaf microperforated panel absorbers. Applied Acoustics 2006; 67: 609-619.
[18] Sakagami K, Nakamori T, Morimoto M, Yairi M. Double-leaf microperforated panel space absorbers: A revised theory and detailed analysis. Applied Acoustics 2009; 70: 703-709.
[19] Sakagami K, Morimoto M, Yairi M. Application of microperforated panel absorbers to room interior surfaces. Int. J. Acoust. Vib. 2008; 13: 120-124.
[20] Sakagami K, Yamashita I, Yairi M, Morimoto M. Sound absorption characteristics of a honeycomb-backed microperforated panel absorber: revised theory and experimental validation. Noise Control Eng. J. 2010; 58: 157-162.

Captions of figures

Fig.1 The model for theoretical analysis for the case with the microperforated panel (MPP) on the illuminated side (MPP-PM structure).

Fig.2 The model for theoretical analysis for the case with the permeable membrane (PM) on the illuminated side (PM-MPP structure).

Fig.3. Sound absorbing structures to be compared with the MPP-PM structure. (a) MPP－PM structure, (b) double-leaf MPP structure with a back wall, (c) single-leaf MPP structure with a back wall.

Fig.4. Calculated result of the field-incidence-averaged absorption coefficient of the MPP-PM structure in comparison with that of other absorption structures in Fig. 3. Thick line: MPP-PM structure, Thin line: common single-leaf MPP, and Dashed line: common double-leaf MPP. Parameters: MPP : t=0.3mm, d=0.3mm, p=1.0%, M_{MPP}=1.0kg/m^2. PM : R=816Pa s/m, M_{PM}=1.0kg/m^2, D_1=D_2=50mm

Fig.5. Configurations of common single-leaf MPP absorbers to be compared with the MPP-PM structure. (a) MPP－PM structure, (b) common single-leaf MPP with air-cavity of 100 mm deep, (c) common single-leaf MPP with air-cavity of 50mm deep.

Fig.6. Comparison of the MPP-PM structure with common single-leaf MPP absorbers (normal incidence). Thick line: MPP-PM, Thin line: single-leaf MPP with 100 mm air cavity, and Dashed line: single-leaf MPP with 50 mm air cavity. Parameters are the same as those in Fig. 4.

Fig.7. Sound absorbing structures to be compared with the PM-MPP structure. (a) PM-MPP structure, (b) double-leaf MPP structure with a back wall, (c) single-leaf MPP structure with a back wall.

Fig.8. Calculated result of the field-incidence-averaged absorption coefficient of the PM-MPP structure in comparison with that of other absorption structures in Fig. 7. Thick line: PM-MPP, Thin line: single-PM, and Dashed line: double-leaf MPP.

Fig.9. Configurations of common single-leaf MPP absorbers to be compared with the PM-MPP structure. (a) PM-MPP structure, (b) common single-leaf MPP with air-cavity of 100 mm deep, (c) common single-leaf MPP with air-cavity of 50mm deep.

Fig.10. Comparison of the PM-MPP structure with common single-leaf PM absorbers (normal incidence). Thick line: PM-MPP structure, Thin line: single-PM with 100 mm air cavity, and Dashed line: single-PM with 50 mm air cavity. Parameters are the same as those in Fig. 4.

Fig.11. Sketches of the honeycomb inserted in the air cavities of the MPP-PM structure. (a) without honeycomb, (b) honeycomb inserted in the air cavity D_1, (c) honeycomb inserted in the air cavity D_2, (d) honeycomb inserted in the both cavities.

Fig.12. Effect of the honeycomb in the air cavity of the MPP-PM structure. Parameters are the same as those in Fig. 4. Curves with (a)…(d) correspond to the configurations (a)…(d) in Fig. 11, respectively.

Fig.13. Sketches of the honeycomb inserted in the air cavities of the PM-MPP structure. (a) without honeycomb, (b) honeycomb inserted in the air cavity D_1, (c) honeycomb inserted in the air cavity D_2, (d) honeycomb inserted in the both cavities.

Fig.14. Effect of the honeycomb in the air cavity of the PM-MPP structure. Parameters are the same as those in Fig. 4. Curves with (e)…(h) correspond to the configurations (e)…(h) in Fig. 13, respectively.

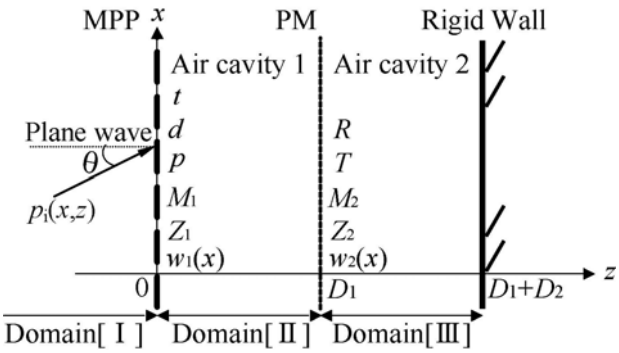

Fig.1 The model for theoretical analysis for the case with the microperforated panel (MPP) on the illuminated side (MPP-PM structure).

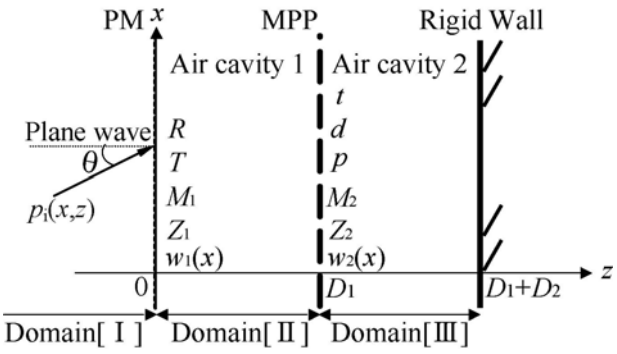

Fig.2 The model for theoretical analysis for the case with the permeable membrane (PM) on the illuminated side (PM-MPP structure).

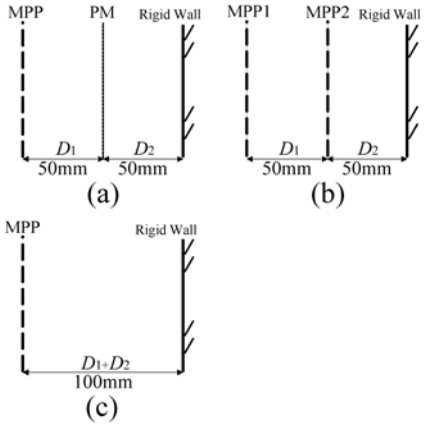

Fig.3. Sound absorbing structures to be compared with the MPP-PM structure. (a) MPP－PM structure, (b) double-leaf MPP structure with a back wall, (c) single-leaf MPP structure with a back wall.

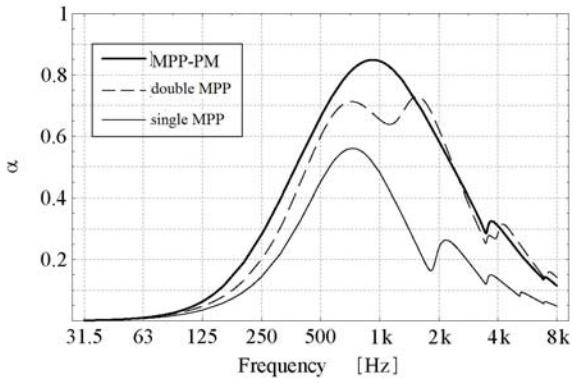

Fig.4. Calculated result of the field-incidence-averaged absorption coefficient of the MPP-PM structure in comparison with that of other absorption structures in Fig. 3. Thick line: MPP-PM structure, Thin line: common single-leaf MPP, and Dashed line: common double-leaf MPP. Parameters: MPP : t=0.3mm, d=0.3mm, p=1.0%, M_{MPP}=1.0kg/m^2. PM : R=816Pa s/m, M_{PM}=1.0kg/m^2, D_1=D_2=50mm

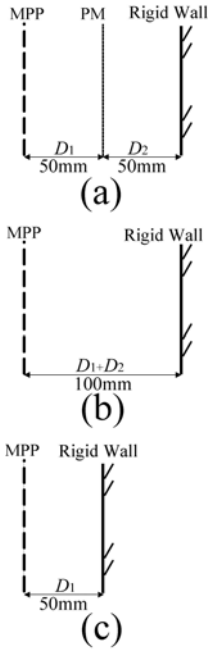

Fig.5. Configurations of common single-leaf MPP absorbers to be compared with the MPP-PM structure. (a) MPP－PM structure, (b) common single-leaf MPP with air-cavity of 100 mm deep, (c) common single-leaf MPP with air-cavity of 50mm deep.

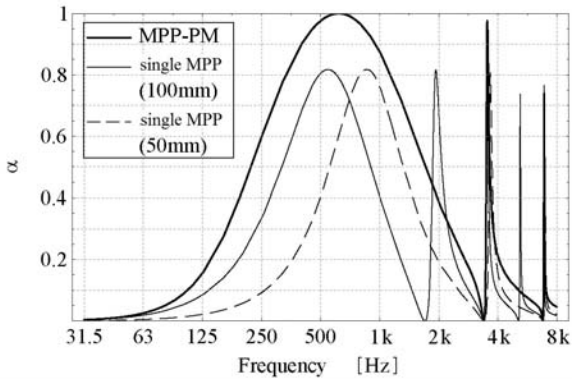

Fig.6. Comparison of the MPP-PM structure with common single-leaf MPP absorbers (normal incidence). Thick line: MPP-PM structure, Thin line: single-leaf MPP with 100 mm air cavity, and Dashed line: single-leaf MPP with 50 mm air cavity. Parameters are the same as those in Fig. 4.

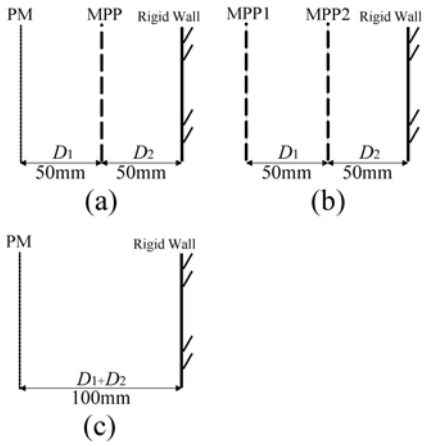

Fig.7. Sound absorbing structures to be compared with the PM-MPP structure. (a) PM-MPP structure, (b) double-leaf MPP structure with a back wall, (c) single-leaf MPP structure with a back wall.

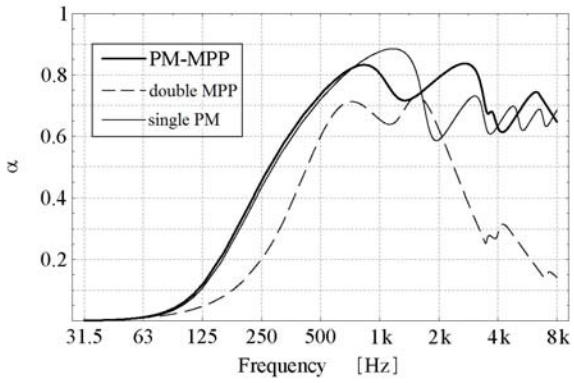

Fig.8. Calculated result of the field-incidence-averaged absorption coefficient of the PM-MPP structure in comparison with that of other absorption structures in Fig. 7. Thick line: PM-MPP structure, Thin line: single-PM, and Dashed line: double-leaf MPP.

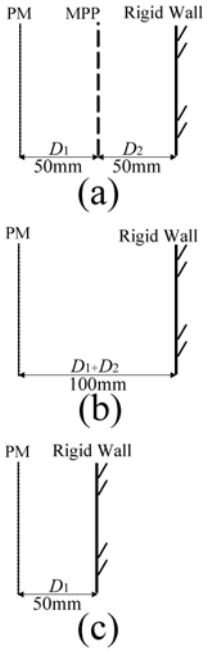

Fig.9. Configurations of common single-leaf MPP absorbers to be compared with the PM-MPP structure. (a) PM-MPP structure, (b) common single-leaf MPP with air-cavity of 100 mm deep, (c) common single-leaf MPP with air-cavity of 50mm deep.

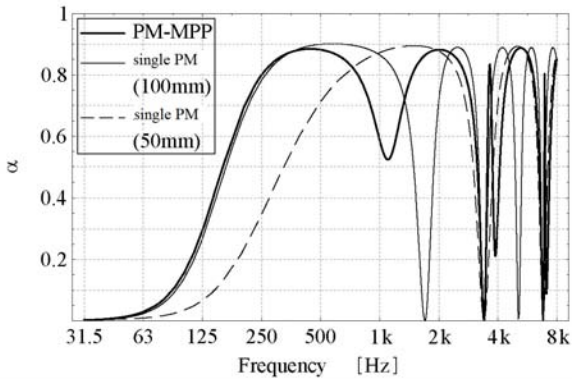

Fig.10. Comparison of the PM-MPP structure with common single-leaf PM absorbers (normal incidence). Thick line: PM-MPP structure, Thin line: single-PM with 100 mm air cavity, and Dashed line: single-PM with 50 mm air cavity. Parameters are the same as those in Fig. 4.